Importance of Intracellular Fe Pools on Growth of Marine Diatoms by Using Unialgal Cultures and the Oyashio Region Phytoplankton Community during Spring

Koji Sugie[1, 2, *], Kenshi Kuma[1, 3], Satoshi Fujita[1], Satomi Ushizaka[1], Koji Suzuki[1, 4] and Tsutomu Ikeda[3]

[1] Graduate School of Environmental Science, Hokkaido University, North 10 West 5, Kita-ku, Sapporo, Hokkaido 060-0810, Japan

[2] Present address: Central Research Institute of Electric Power Industry, 1646 Abiko, Abiko, Chiba 270-1194, Japan

[3] Faculty of Fisheries Sciences, Hokkaido University, 3-1-1 Minato-cho, Hakodate, Hokkaido 041-8611, Japan

[4] Faculty of Environmental Earth Science, Hokkaido University, North 10 West 5, Kita-ku Sapporo, Hokkaido 060-0810, Japan

*AUTHOR for CORRESPONDENCE:

Koji Sugie E-mail: kojisugie@gmail.com

Central Research Institute of Electric Power Industry, 1646 Abiko, Abiko-shi, Chiba 270-1194, Japan

Tel: +81-4-7183-2966, Fax: +81-4-7183-8291

Key words

Fe storage; intracellular Fe; luxury Fe uptake; centric diatoms; survival strategy

Running Head

Utilizing intracellular Fe by diatoms

Abstract: We report on the ability for luxury Fe uptake and the potential for growth utilizing intracellular Fe pools for 4 coastal centric diatom isolates and *in situ* phytoplankton assemblages, mainly composed of diatoms. Iron uptake of the diatom isolates and natural phytoplankton assemblages in the Oyashio region during spring blooms were prevented by adding hydroxamate siderophore desferrioxamine B (DFB). After the addition of DFB, intracellular Fe in the diatom isolates supported 2.4–4.2 cell divisions with 1.2–2.6 Chl *a* doublings. The intracellular Fe was primarily used for cell generation rather than Chl *a* production, leading to a reduction in the Chl *a* cell quota in the Fe-starved cells with time. The metabolic properties of the Fe-starved cells with their cell morphologies were different among species or genera. An on-deck incubation experiment also exhibited 1.9 cell divisions and 0.81 Chl *a* doublings of phytoplankton after the addition of DFB also indicating the preference of cell generation over Chl *a* production. A decrease in the level of cellular Chl *a*, a main light-harvesting pigment in Fe-starved diatoms may become a superior survival strategy to protect the cells from high irradiance that can cause photo-oxidative damages through photosynthesis. Such relatively low-Fe with high-light conditions could often occur in surface waters of the Oyashio region from spring to summer.

1 Introduction

Over the last few decades, many studies have shown iron (Fe) to be the most important micronutrient for marine phytoplankton growth, because of its role in key metabolic processes such as photosynthesis, respiration, and nitrate and nitrite assimilations (Geider and Roche, 1994; Raven et al., 1999). The Fe acquisition by phytoplankton is strongly influenced by seawater chemistry and speciation in seawater (Morel et al., 2008). In oxic seawater, Fe is present predominantly in the insoluble (extremely low solubility) and thermodynamically stable 3+ oxidation state (Kuma et al., 1996; Stumm and Morgan, 1996). The rate of Fe uptake by phytoplankton is related to the computed equilibrium concentration of Fe^{3+} in seawater; this uptake is dependent on the concentration of dissolved inorganic Fe(III) species (Fe(III)′), which is proportional to [Fe^{3+}] (Anderson and Morel, 1982; Hudson and Morel, 1990; Sunda, 2001). However, there are apparent exceptions to this model. One of these involves the specific transport of Fe complex with organic ligands such as siderophores that could be indirectly and/or directly utilized by the cells (e.g. Hutchins et al., 1999a; Maldonado and Price, 2001; Sunda, 2001; Hassler et al., 2011). Shaked et al. (2005) proposed a new model for Fe uptake by diatoms in which the extracellular enzymatic reduction of all Fe species is a necessary step; this model has recently been supported by molecular assay (e.g. Kustka et al., 2007).

Eukaryotic mechanisms of Fe uptake from siderophore binding Fe are mostly involved in cell surface metalloreductases, whereas prokaryotes can acquire Fe from siderophore-Fe complexes directly through plasma membrane (Yun et al., 2000; Allen et al., 2008; Terzulli and Kosman, 2010). However, Fe uptake of the marine phytoplankton communities have often been almost diminished by adding excess concentrations of the siderophore desferrioxamine B (DFB) compared to Fe in seawater (e.g. Wells et al., 1994; Hutchins et al., 1999b; Wells, 1999). DFB is a small trihydroxamate molecule that complexes inorganic Fe(III) with an extremely high conditional stability constant ($K'_{FeL,Fe(III)}$ = [Fe(III)L]/[Fe(III)][L′] = $10^{16.5}$ M^{-1}; Hudson et al., 1992). Other studies reported lower $K'_{FeL,Fe(III)}$ values between $10^{12.1}$ and $>10^{13.0}$ of DFB-Fe complex with cathodic stripping voltammetry (CSV). However, these experiments were probably conducted by using inappropriate methods or conditions such as using weak competing ligand of salicylaldoxime (Rue and Bruland, 1995) or under lower pH condition than in seawater (Witter et al., 2000). Croot and Johnson (2000) supported a high value of $K'_{FeL,Fe(III)}$ of DFB-Fe complex ($10^{16.5}$ M^{-1}) measured

by CSV using 2-(2-thiazolylazo)-p-cresol as a competing ligand at pH 8.0. The pennate diatom *Phaeodactylum tricornutum* grown under Fe-limited condition can acquire Fe from DFB-Fe complex by reducing the complex via cell surface metalloreductases and subsequent transport Fe into the cell (Soria-Dengg and Horstmann, 1995; Allen et al., 2008). However, the reduction and subsequent uptake of Fe from DFB-Fe complex by marine diatoms is generally orders of magnitude lower than that with Fe(III)′, especially under Fe-sufficient conditions (Maldonado and Price, 2001; Morel et al., 2008). Recent culture experiments have demonstrated that DFB regulates Fe availability by preventing Fe uptake from the ambient extracellular medium (Iwade et al., 2006; Yoshida et al., 2006). Coastal centric diatoms (*Chaetoceros socialis* and *Thalassiosira weissflogii*) maintained their high growth rate for a few days after DFB addition by utilizing their intracellular Fe and the Fe supported up to 2–3 cell divisions without any additional Fe uptake (Iwade et al., 2006). Iwade et al., (2006) also demonstrated by culture and model experiments that the intracellular Fe in *C. socialis* is utilized until critical threshold of their cellular Fe concentration. It has been observed that oceanic and coastal eukaryotic phytoplankton can accumulate excess Fe (which we defined as 'stored Fe' in the present study) compared to the Fe requirement fulfilling their maximum growth rate when the concentration of bioavailable [Fe(III)′] is high; i.e., luxury uptake (Sunda and Huntsman, 1995, 1997). In the Fe-replete coastal environment, Wells (1999) suggested that larger cells (>5 μm) can sustain carbon uptake at least for several hours after the DFB addition probably due to utilizing intracellular Fe reservoir, whereas the smaller cells (<5 μm) seem less storage Fe intracellularly. The pennate diatom *Pseudo-nitzschia* species has recently been found to possess ferritin as an Fe storage protein which accumulate Fe under Fe-replete condition (Marchetti et al., 2009). *Pseudo-nitzschia* species can increase in cell number several times higher than the centric oceanic-diatom *Thalassiosira oceanica*, which does not encode ferritin (Armbrust et al., 2004; Marchetti et al., 2009). It is also known that *P. tricornutum* can also greatly reduce their Fe requirement (e.g. Kustka et al., 2007) resulting by downregulate the processes that require Fe such as photosynthesis, mitochondorial electron transport and nitrate assimilation (Allen et al., 2008). On the other hand, *Chlamydomonas reinhardtii* (Chlorophyceae) synthesize ferritin under Fe-deficient conditions binding intracellular Fe released from PS I to protect photooxidative stress (Busch et al., 2008). Although a few studies suggested that the centric diatom species seems to store Fe intracellularly, there is little explanation about the mechanism of Fe storage and subsequent

utilization in the centric diatom.

In the Oyashio region, western subarctic North Pacific Ocean dissolved Fe concentration change seasonally; the dissolved Fe concentration increased up to ~0.5–1 nmol L^{-1} by deep mixing during winter and decreased below ~0.1–0.2 nmol L^{-1} during summer due to intensive biological activities during spring bloom period (Nishioka et al., 2007). Recent studies demonstrated that the dissolved and total dissolvable Fe concentrations in the upper mixed layer varied an order of magnitude mainly due to vertical and horizontal water mass mixing in the Oyashio region during spring (Hattori-Saito et al., 2010; Nakayama et al., 2010; Sugie et al., 2010a). Therefore, it can be assumed that the phytoplankton, especially diatoms in the Oyashio spring bloom community need to survive under frequently fluctuated Fe environment during spring and under lowering Fe concentrations toward summer.

In the present study, we investigated the ability of luxury Fe uptake and growth by utilizing intracellular Fe for 4 coastal centric diatoms. The coastal diatoms we selected were ecologically and biologically important species of *Thalassiosira nordenskioeldii* and *Thalassiosira anguste-lineata* in subarctic to boreal regions (Sugie et al., 2010a, 2010b), and of *Skeletonema costatum* s.l. and *T. weissflogii* in temperate regions; the Fe storage and subsequent utilization in the former 3 species are examined for the first time. We also investigated their ability to grow by utilizing intracellular Fe in a natural phytoplankton community in the Oyashio region. We conducted a shipboard incubation with or without the addition of DFB into surface water relatively high in Fe and macronutrients during spring blooms.

2 Materials and Methods

2. 1 Laboratory culture experiments

The 4 coastal diatom species used were *T. nordenskioeldii* (isolated from the Oyashio region by author Sugie K.), *T. anguste-lineata* (the same authority as *T. nordenskioeldii*), *Skeletonema costatum* s.l. (unknown authority), and *T. weissflogii* (CCMP 1336). Diatoms were grown at either 10°C (*T. nordenskioeldii* and *T. anguste-lineata*) or 20°C (*S. costatum* s.l. and *T. weissflogii*) under 150 µmol photon m^{-2} s^{-1} fluorescent light (12 h light : 12 h dark) throughout this

study. Seawater for culture media was collected from a coastal region in the northern Japan Sea near Hokkaido, Japan, and filtered through an acid-cleaned 0.22 μm Millipore membrane filter. Filtered seawater was autoclaved for 20 min at 121°C (108 kPa). The concentrations of Fe, NO_3+NO_2, NH_3, PO_4, and $Si(OH)_4$ in the autoclaved filtered seawater were less than 2 nmol L^{-1}, 6, 0.1, 0.4, and ~240 μmol L^{-1}, respectively. Prior to the culture experiments, four centric diatoms were grown in silicate enriched f/2 medium (silicic acid enriched f/2 nutrient plus f/2 metals to the autoclaved filtered seawater) (Guillard and Ryther, 1962), with at least two transfers and more than 18-doublings at the exponential growth phase. The silicic acid enriched f/2 medium contained 886 μmol L^{-1} NO_3, 38 μmol L^{-1} PO_4 and ~350 μmol L^{-1} $Si(OH)_4$ as macronutrients, and 11.7 μmol L^{-1} Fe(III), 0.44 μmol L^{-1} Co(II), 0.91 μmol L^{-1} Mn(II), 73 nmol L^{-1} Zn(II), 28 nmol L^{-1} Cu(II), and 29 nmol L^{-1} Mo(VI) with 15 μmol L^{-1} EDTA as essential metals. All f/2 nutrient stock solutions were passed through Chelex 100 ion-exchange resin to remove trace metals (Morel et al., 1979). Diatoms at the late exponential growth phase in f/2 medium were inoculated into modified f/2 medium, which was prepared without adding any trace metals, EDTA, nor vitamins to the f/2 medium, before the culture experiment to obtain slightly Fe stressed cells. The diatoms were acclimated in the Fe- and manganese (Mn)-added modified f/2 media, to which ferric Fe stock solution (25 μmol L^{-1} Fe(III): $FeNH_4(SO_4)_2 \cdot 12H_2O$ in 5 mmol L^{-1} HCl, pH 2.3) and Mn stock solution (25 μmol L^{-1} Mn(II): $MnCl_2$ in 5-mmol L^{-1} HCl, pH 2.3) were added to make Fe and Mn concentrations of 100 nmol L^{-1} and 25 nmol L^{-1}, respectively. Previous studies have found that the addition of both Mn and Fe to the modified f/2 medium kept the cells in physiologically good state for a suitable length of time (Peers and Price, 2004; Ushizaka et al., 2008). Hence, we added Mn to the culture media in the present study.

We used DFB to prevent the further Fe uptake from ambient extracellular Fe in the media as demonstrated before (Iwade et al., 2006; Yoshida et al., 2006). The bacterial hydroxamate siderophore DFB (Sigma Chem. Co. Ltd.), forming a 1:1 DFB-Fe(III) complex, was stored in the dark under frozen condition until further use. A premixed DFB-Fe(III) complex medium (Table 1) was prepared by mixing small amounts of acidic ferric Fe and DFB stock (1 mmol L^{-1}) solutions at a DFB:Fe molar ratio of 10:1 in a pre-cleaned polycarbonate Erlenmeyer flask. Then, modified f/2 medium (50 mL) was added, and diatoms inoculated [premix DFB-Fe(III) treatment]. The final Fe, Mn, and DFB concentrations in the premixed DFB-Fe(III) medium were 100 nmol L^{-1}, 25 nmol L^{-1},

and 1 μmol L^{-1}, respectively, and the calculated [Fe(III)′] was 3.5 amol L^{-1}. A control medium (DFB treatment) containing DFB and Mn at a final concentration of 1 μmol L^{-1} and 25 nmol L^{-1} without Fe in the modified f/2 medium was used to examine the bioavailability of the DFB-Fe complex (premixed DFB-Fe media). The Fe-replete condition was examined by simultaneously adding small amounts of acidic ferric Fe and Mn stock solutions (final Fe concentrations of 10 and 100 nmol L^{-1}, and final Mn concentration of 25 nmol L^{-1}) and each diatom species into the modified f/2 media [direct Fe(III)-10 and direct Fe(III)-100 treatments]. Growth by utilizing intracellular Fe was examined by adding DFB to a final concentration of either 0.1 or 1-μmol L^{-1} [DFB:Fe(III) = 10:1] after 1 and/or 3 days of cultivation in direct Fe(III) input media to allow the diatoms uptake Fe under various [Fe(III)′] conditions until DFB addition [direct Fe-10-DFB-1 d or direct Fe-100-DFB-1 d and/or direct Fe-100-DFB-3 d treatments]. Culture experiments for *T. anguste-lineata* were not carried out in direct Fe(III)-10 and direct Fe-10-DFB-1 d treatments (Table 1). Cell concentrations at the beginning of culture experiments were approximately 1,000 cells mL^{-1}. The light, temperature, and macronutrient conditions were the same as those of the stock culture described earlier. Culture experiments were conducted in triplicate but in duplicate for controls and premixed DFB-Fe(III) treatments.

Cell growth was monitored daily by triplicate cell counts done with an optical microscope. Cell sizes were measured using an optical microscope with a calibrated ocular micrometer for at least 20 cells of each chain at the beginning and the end of the culture experiments; the cell volume (CV) and surface area (SA) were calculated according to the geometric shape suggested by Hillebrand et al. (1999) and Sun and Liu (2003). The daily Chl *a* concentrations were measured with a fluorometer (Turner Designs 10-AU) according to the method of Welschmeyer (1994), after adding 100–200 μL of cultivation directly into a quartz cuvette with 5 mL of *N*, *N*-dimethylformamide (DMF; Suzuki and Ishimaru, 1990), and extraction in the dark for 4-h at room temperature. All bottles, flasks, and tubes used in culture experiments were acid-washed (soaked for at least 24 h in either 1 or 4 mol L^{-1} HCl solution; 1 mol L^{-1} HCl was used for polycarbonate apparatus) and then repeatedly rinsed with Milli-Q water (>18.0 MΩ cm^{-1}, Millipore). The preparation and sampling for the experiments were conducted in a Class 100 laminar flow cabinet to avoid inadvertent trace metal contamination.

211 2. 2 Shipboard incubation experiment

212 Shipboard incubation of phytoplankton communities was conducted using surface water
213 of the Oyashio region of the western subarctic Pacific Ocean. These experiments were part of the
214 Ocean Ecodynamics Comparison in the Subarctic Pacific (OECOS) project aboard R/V
215 Hakuho-Maru (KH-07-01 cruise). Near-surface seawater (10 m depth) was collected during the
216 spring bloom on 6 April 2007, from Oyashio waters (low temperature of 1.70°C and low salinity of
217 33.04) at 42°00′N and 145°15′E using acid-cleaned, Teflon-coated, 10-L Niskin X sampling bottles
218 (General Oceanics) attached to a CTD-CMS.

219 All incubation apparatuses used in the shipboard experiment were rigorously acid-washed
220 and Milli-Q rinsed according to Takeda and Obata (1995). All the preparations for the shipboard
221 incubation were performed in a clean room or on a clean bench (Class 100). After sieving with a
222 100 μm acid-cleaned Teflon-mesh to eliminate mesozooplankton, seawater samples were
223 homogenized in a 20 L acid-washed polyethylene tank and dispensed immediately into 250 mL
224 acid-washed polycarbonate incubation bottles. The ability of natural phytoplankton growth by
225 utilizing intracellularly stored Fe was examined by adding DFB to the incubation bottles (DFB
226 treatment). The final DFB concentration was set at 1 μmol L^{-1}, a value that is likely to be
227 approximately 2–4 orders of magnitude higher than that of Fe in natural oceanic seawater. An
228 unamended control was prepared to allow phytoplankton uptake ambient extracellular Fe and to
229 compare the growth of DFB treatment. Triplicate incubation bottles for each treatment and for the
230 samplings on 1, 3, and 5 day incubations were placed at 5°C in an incubator under 150 μmol
231 photons m^{-2} s^{-1} fluorescent light (12 h light : 12 h dark). Temperature and light intensity were
232 within the entire range observed from 1 to 6°C and 13 to 36% of the surface irradiance, respectively
233 (Isada et al., 2010; Sugie et al., 2010a). Bottles were sacrificed at each sampling point. Chl *a*
234 concentrations were measured at the beginning and after 1, 3, and 5 days of incubation. Seawater
235 was filtered onto 0.45 μm omnipore membrane filter (Millipore) and pigments on the filter samples
236 were extracted in DMF (Suzuki and Ishimaru, 1990). The analytical procedure was the same as that
237 described earlier. Diatom cell counts and species composition analysis were performed only at the
238 beginning and after 5 days of incubation using a phase-contrast inverted microscope (Hasle and
239 Syvertsen, 1997). Samples of the replicates were mixed together with the same volume and then
240 fixed with neutralized formalin at a final concentration of 1 % (Hasle, 1978). The Fe concentration

of filtered (<0.22 μm: labile dissolved Fe) and unfiltered (total dissolvable Fe) natural seawater was determined by an automated Fe analyzer (Kimoto Electric) with a combination of chelating resin concentration and luminol-hydrogen peroxide chemiluminescence detection in a closed flow-through system (Obata et al., 1993). The concentration of macronutrients in the seawater samples were measured with a QuAAtro continuous flow analyzer (Bran+Luebbe).

3 Results

3.1 Laboratory unialgal culture experiments

No nutrient depletion was detected during the incubation experiment even for *S. costatum* s.l. in direct Fe(III)-100 treatment being the growth ceased at the end when the concentrations were NO_3+NO_2 ~300 μmol L^{-1}, PO_4 4–9 μmol L^{-1} and $Si(OH)_4$ >150 μmol L^{-1}. In 3 of the 4 species (the exception being *S. costatum* s.l.), there were significant decreases (approximately 10–15%) in both CV and SA ($p < 0.01$, 1-way ANOVA) during 7–9 day incubation periods under the Fe-starved conditions by adding DFB (Table 2). The CV and SA of *S. costatum* s.l. increased after 6 day of Fe-starved incubation with 1.5–1.7-fold higher than the values at the beginning of the experiment ($p < 0.01$, 1-way ANOVA). A slight increase in surface area to cell volume ratio (SA/CV) with Fe-starved incubation was observed for all 4 species (Table 2).

For all 4 species there was no difference in either cell density or Chl *a* concentration between control (DFB only) and premixed DFB-Fe media (Figs. 1–4). Direct Fe(III)-100 input medium induced the highest maximal cell and Chl *a* yields (Figs. 1–5). The relative order of maximal cell yields for *T. nordenskioeldii* (10°C) in different culture media was as follows: direct Fe(III)-100 = direct Fe(III)-10 (~95,000 cells mL^{-1}) > direct Fe-100-DFB-1d (47,000 cells mL^{-1}) > direct Fe-10-DFB-1d (35,000 cells mL^{-1}) >> premixed DFB-Fe(III) = control (~7,600 cells mL^{-1}). For *T. anguste-lineata* (10°C) the relative order of maximal cell yields was as follows: direct-Fe(III)-100 (27,000 cells mL^{-1}) > direct Fe-100-DFB-1d (14,000 cells mL^{-1}) >> premixed DFB-Fe(III) = control (~7,100 cells mL^{-1}). However, maximal cell yields for *S. costatum* s.l. and *T. weissflogii* (20°C) were clearly higher in direct Fe(III)-100 medium (1,960,000 cells mL^{-1} for *S. costatum* s.l. and 442,000 cells mL^{-1} for *T. weissflogii*) than in direct Fe(III)-10 medium (454,000 cells mL^{-1} for *S. costatum* s.l. and 172,000 cells mL^{-1} for *T. weissflogii*) (Figs. 3a-1 and 4a-1). The relative order of maximal Chl *a* concentrations for all diatom species was as follows: direct

Fe(III)-100 > direct Fe(III)-10 > direct Fe-100-DFB-1d > direct Fe-10-DFB-1d >> premixed DFB-Fe(III) = control (DFB). For *T. nordenskioeldii*, *S. costatum* s.l. and *T. weissflogii*, the maximal Chl *a* concentration in the direct Fe(III)-10 medium was about half, one tenth and one thirds, respectively of those in the direct Fe(III)-100 medium (Figs. 1b-1, 3b-1 and 4b-1).

Even after the addition of DFB, cell density in the direct Fe-DFB-1d media increased for 4–5 days for *S. costatum* s.l. and *T. weissflogii* and 6 days for *T. nordenskioeldii* and *T. anguste-lineata* (Figs. 1a-2, 2a-2, 3a-2 and 4a-2). However, Chl *a* concentrations increased only for ~2 days for *S. costatum* s.l. and *T. weissflogii* and <5 days for *T. nordenskioeldii* and *T. anguste-lineata* after the addition of DFB (Figs. 1b-2, 2b-2, 3b-2 and 4b-2). The cell specific growth rates for 2–3 days after addition of DFB were the same as those in the direct Fe(III)-100 media, whereas the Chl *a* specific growth rates were decreased within 1–2 days after the addition of DFB. The relative increase in cell doublings [$\log_2$ (maximal cell density after DFB addition divided by the cell density at DFB addition on 1 or 3 day of cultivation)] was lower in direct Fe-100-DFB-3 d media (3.2, 1.2, 3.4 and 3.1 doublings for *T. nordenskioeldii*, *T. anguste-lineata*, *S. costatum* s.l. and *T. weissflogii*, respectively) than in direct Fe-100-DFB-1 d media (4.2, 2.5, 4.1 and 3.3 fold for *T. nordenskioeldii*, *T. anguste-lineata*, *S. costatum* s.l., *T. weissflogii*, respectively) (Fig. 5). The intracellular Fe in direct Fe-100-DFB-1d medium supported up to 2.5–4.2 cell divisions and a maximum of 1.2–2.6 Chl *a* doublings [$\log_2$ (maximal Chl *a* concentration after DFB addition divided by Chl *a* concentration at DFB addition)] (Fig. 6). The relative order of Chl *a* doublings was *S. costatum* s.l. ≈ *T. weissflogii* (2.5–2.6) > *T. nordenskioeldii* (2.3) > *T. anguste-lineata* (1.2) (Fig. 6).

3.2 Growth of in situ phytoplankton utilizing intracellular Fe

The near-surface Oyashio seawater collected for shipboard incubation had high concentrations of labile dissolved (D-Fe), total dissolvable Fe (T-Fe), macronutrients, Chl *a* and diatom abundance [D-Fe, 0.41 nmol L^{-1}; T-Fe, 15.7 nmol L^{-1}; NO_3+NO_2, 20.4 µmol L^{-1}; PO_4, 1.45 µmol L^{-1}; $Si(OH)_4$, 32.3 µmol L^{-1}, Chl *a*, 12.2 µg L^{-1} and ~3,200 cells mL^{-1}]. The high Fe, macronutrients, and Chl *a* concentrations are probably attributed to the lateral surface intrusion of the Coastal Oyashio Water (COW), characterized by low temperature and low salinity (Hanawa and Mitsudera, 1987) into the Oyashio region (Sugie et al., 2010a, Nakayama et al., 2010). The high Chl

301 *a* biomass can be achieved due to the shallow mixed layer depth (~10 m) with high Fe and nutrient
302 concentrations, and the phytoplankton in the water sample used in the present study is considered to
303 be in an exponential to peak of the spring bloom. Mixed layer depth, chemical and phytoplankton
304 properties at the sampling station were temporally changed due to mixing COW, Oyashio Water and
305 modified Kuroshio Water during the KH-07-01 cruise (Kono and Sato, 2010; Sugie et al., 2010a).
306 For example, the concentration of T-Fe macronutrients and Chl *a* varied one order of magnitude in
307 the upper mixed layer, ranging 0.7–25 nmol L^{-1} T-Fe, 1.9–19 μmol L^{-1} NO_2+NO_3, 0.6–1.9 μmol L^{-1}
308 PO_4, and 3.1–36 μmol L^{-1} $Si(OH)_4$ (Nakayama et al., 2010; Sugie et al., 2010a).
309 The Chl *a* concentration of natural phytoplankton assemblages increased over 1–3 days of
310 cultivation, and the net growth rate was faster in control than in DFB treated conditions. The highest
311 Chl *a* concentration was observed at 3 day of incubation with approximately 32 μg L^{-1} in the
312 control and 21 μg L^{-1} in DFB treatment (Fig. 7a-1). The Chl *a* concentration at 5 day of incubation
313 in controls was 1.5-times higher than that seen in DFB treatment, while the diatom cell yields at 5
314 day of incubation in the control was almost the same as those in the DFB treated conditions (Fig.
315 7a-2). Throughout the *in situ* phytoplankton incubations, centric diatoms of *Thalassiosira* spp. and
316 *Chaetoceros* spp. (subgenus *Hyalochaete*) were predominant, accounting for >97% of diatom
317 abundance, with pennate diatoms being only a minor component <2.5% (Fig. 7a-2). Other
318 phytoplankton groups were extremely low dominancy under microscopic observation, and the
319 diatom species were commonly seen in the Oyashio region during spring bloom (Tsuda et al., 2005;
320 Sugie et al., 2010a, 2010b). On day 5 of DFB treatment, diatom cell density had increased to
321 ~12,000 cells mL^{-1} representing 1.9 cell divisions, while the Chl *a* concentration was only 0.81
322 doublings. Macronutrient concentrations in controls decreased rapidly to nearly zero at 3 day for
323 NO_3+NO_2 and $Si(OH)_4$, and reached and remained ~0.25 μmol L^{-1} during 3–5 day of cultivations
324 for PO_4. Macronutrient concentrations in DFB treatments also decreased rapidly to nearly zero at 3
325 day for NO_3+NO_2 (Fig. 7b-1), remained 0.4 μmol L^{-1} at 5 day for PO_4 (Fig. 7b-2) and 1.4 μmol L^{-1}
326 at 5 day for $Si(OH)_4$ (Fig. 7b-3).
327
328 **4 Discussion**
329 4.1 Changes in cell morphology under Fe-starved conditions
330 Variation in cell morphology may be an important factor influencing the Fe uptake of

diatoms, because a reduction in cell size increases the SA/CV ratio and thereby maximizes transporter uptake rates relative to cellular Fe requirements (Sunda and Huntsman, 1995). Previous studies have found low Fe acclimated Fe-limited and DFB added Fe-starved coastal and oceanic centric diatoms to show a 20–50% decrease in CV, and a resultant increase in SA/CV ratio of 8–26% (Sunda and Huntsman, 1995; Sugie and Kuma, 2008). In addition, it has been reported that the Fe-limited cells of the marine pennate diatom *Pseudo-nitzschia* spp. acclimatize to low Fe concentrations with a reduction in CV of 14–44% and an increase in SA/CV ratio of 9–40% (Marchetti and Harrison, 2007). Similarly, 3 out of the 4 diatom species cultured in the present study showed reduction in CV and SA (of 15–20% and 8.5–14%, respectively) in Fe-starved conditions produced by the addition of DFB (direct Fe-100-DFB 1 d medium). These reductions were associated with an increase in SA/CV ratio of 7–8% (Table 2) but the change was smaller than that of *Pseudo-nitzschia* spp. reported by Marchetti and Harrison (2007). In contrast, Fe-starved *S. costatum* s.l. (the smallest diatom species we investigated) exhibited increases in CV of 66% and SA of 68%, and subsequently a slight increase in SA/CV ratio of ~3% (Table 2). It is thus evident that species and/or genera differ in the extent to which they can alter their cellular dimensions under Fe-depleted conditions even among coastal diatom species.

4.2 Luxury Fe uptake and growth utilizing intracellular Fe pools

Cell yields and Chl *a* concentrations were identical between controls (DFB only) and DFB-Fe treatment indicating the centric diatom species we used in laboratory experiment can not utilize Fe from the DFB-Fe complex (Figs. 1–4) as reported previously (Iwade et al., 2006; Yoshida et al., 2006; Chen and Wang, 2008). Even if the diatoms we used were able to uptake Fe from DFB-Fe complex via cell surface reductase (Shaked et al., 2005; Kustka et al., 2007; Morel et al., 2008), the amount should have been negligible at the high DFB:Fe molar ratio of 10 with extreme low [Fe(III)′] of ~3.5 amol L^{-1} in this study. Under the presence of DFB, almost all external bioavailable Fe species such as Fe dissolving from particulate Fe and natural organic Fe complexes form the DFB-Fe complex (Iwade et al., 2006). Therefore, the growth of diatoms after the DFB addition can be accomplished by utilizing only intracellular Fe.

The cell growth of all 4 centric diatom species was maintained for 4–6 days after the addition of DFB and the increase in Chl *a* concentrations were maintained for 2–5 days. In addition,

361 the cell growth rates for ~2–3 days after the DFB addition in direct Fe-100-DFB-1 d media were the
362 same as those in direct Fe(III) input media. However, Chl *a* growth rates decreased within 1–2 days
363 after the addition of DFB. Therefore, the stored Fe via the luxury Fe uptake supported only for 1–2
364 days or 1–2 cell divisions. The surplus 2–3 times of cell divisions after the DFB addition considered
365 to be maintained by sharing intracellular functional Fe pools with daughter cells. The Chl *a* cell
366 quota in Fe-depleted DFB added media (e.g. direct Fe-10-DFB-1d, and direct Fe-100-DFB-1d
367 media) tended to decrease logarithmically with time after the DFB addition (Fig. 8). The reduction
368 in Chl *a* cell quota was 57–73% while the reduction in CV was about 10% (Table 2). These results
369 suggest that intracellular Fe was primarily involved in cell generation rather than Chl *a* synthesis. In
370 addition, the decrease in intracellular Chl *a* concentration can alleviate photooxidative stress (e.g.
371 Ledford and Niyogi, 2005) that may offset the decrease in productivity with the increase in
372 probability of survival under Fe-deficient conditions.

373 The 50–90% of intracellular functional Fe in phytoplankton is localized in chloroplast
374 (Raven, 1988). It has been reported that Fe deficiency of the diatoms induces the decreases in Chl *a*
375 cell quota and in photosynthetic protein levels, especially for the most Fe-rich protein of PS I
376 complex (Geider et al., 1993; Davey and Geider, 2001). *Chlamydomonas reinhardtii*
377 (Chlorophyceae) optimize photosynthetic apparatus by changing the stoichiometry of electron
378 transfer proteins to minimize photooxidative damage under Fe-depleted conditions (Moseley et al.,
379 2002). Busch et al. (2008) reported that the ferritin bind with Fe released from degrading
380 photosynthetic apparatuses such as PS I under Fe-depleted condition by using *C. reinhardtii* and
381 that the ferritin binding Fe is probably redistributed within a cell in response to extracellular Fe
382 conditions. In contrast, pennate diatoms upregulate the ferritin gene under Fe-replete conditions to
383 accumulate Fe intracellularly (Marchetti et al., 2009). However, any examined centric diatoms do
384 not have ferritin gene (e.g. *Thalassiosira pseudonana*; Armbrust et al., 2004). The vacuole is known
385 to store Fe in yeast and higher plants (e.g. Brait et al., 2007), however, the role of vacuole as an Fe
386 storage mechanism in the centric diatoms is unclear (Raven, 1997; Kustka et al., 2007). In the
387 present study, the Fe-binding agent and transporter of the centric diatoms under Fe-sufficient and
388 deficient conditions could not be specified. Then we speculate Fe storage mechanisms in the centric
389 diatoms that (1) the centric diatoms have a specific protein other than ferritin for Fe-storage under
390 Fe-sufficient environment, or (2) Fe-containing proteins in the photosynthetic apparatus (e.g. PS I,

391 PS II, cytochrome b_6-*f*-FeS complex, and ferredoxin; Raven et al., 1999) act as part of an
392 intracellular Fe-storage mechanism.

393 In general, Ti(III)-citrate-EDTA solution (Hudson and Morel, 1989, 1990) has been used
394 to rapidly remove extracellularly absorbed iron by reductive dissolution of Fe(III) for the iron
395 uptake measurement. In our previous studies (Kuma and Matsunaga, 1995; Kuma et al., 2000;
396 Iwade et al., 2006), however, aged amorphous Fe(III) hydroxide produced in direct Fe(III) input
397 during aging above 1 day at 10°C and higher temperature was not completely dissolved by the
398 reductive dissolution with Ti(III) treatment because of the much slower dissolution rate of aged
399 amorphous Fe(III) hydroxide. The dissolution rates of the amorphous Fe(III) hydroxide phase
400 decrease rapidly with aging time and temperature because of the conversion to more stable phase
401 (Kuma and Matsunaga, 1995). Therefore, intracellular Fe concentrations were not measured for >1
402 week duration incubated under 10 and 20°C of the present culture experiments. In the previous
403 studies (Kuma et al., 1999, 2000; Iwade et al., 2006), the direct input of concentrated acidic Fe(III)
404 stock solution into culture media elevates the concentration of bioavailable Fe(III) above the
405 equilibrium concentration (~0.1 nmol L^{-1}) with solid Fe(III) hydroxide in seawater (Kuma et al.,
406 1996), indicating the higher rates of Fe uptake and phytoplankton growth. In addition, the high Fe
407 uptake rate by phytoplankton was accomplished by the high concentration of the freshly hydrolytic
408 precipitated Fe(III) hydroxide with the higher dissolution rate compared to more stable crystal
409 structure of Fe(III) hydroxide species (Kuma and Matsunaga, 1995). The Fe(III) solubility and
410 dissolution rate of solid Fe(III) hydroxide in seawater can limit the uptake of Fe by phytoplankton if
411 the dissolution rate is slow in relation to the further demands of phytoplankton. The maximal cell
412 yields and growth rates in direct Fe(III) input media were higher in direct Fe(III)-100 media than
413 direct Fe(III)-10 media (Figs. 1–5). It is likely that the dissolution of solid amorphous Fe(III)
414 hydroxide with 100 nmol L^{-1} in culture media is sufficiently larger to accomplish the maximal cell
415 yields and the high growth rate than that with 10 nmol L^{-1}, suggesting smaller supply of
416 bioavailable Fe(III) in the Fe(III)-10 media compared to the Fe(III)-100 media. In addition, the
417 higher cell divisions and Chl *a* doublings after DFB addition in the direct Fe-100-DFB 1 d media
418 than in the direct Fe-100-DFB 3 d media were probably due to the higher dissolution rate of the
419 freshly precipitated solid Fe(III) hydroxide than the aged solid Fe(III) hydroxide (Fig. 6; Kuma and
420 Matsunaga, 1995; Yoshida et al., 2006).

421

422 4.3 Growth of in situ phytoplankton utilizing intracellular Fe

423 Our field incubation study demonstrated the 1.9 divisions and the 0.81 Chl *a* doublings of
424 diatoms with nitrate exhaustion even after the addition of DFB. If *in situ* labile dissolved Fe bound
425 with added DFB, [Fe(III)'] is calculated to be 0.013 amol L^{-1}. Bioavailable fraction of total
426 dissolvable Fe will also complex with DFB, and hence, [Fe(III)'] is 0.68 amol L^{-1} at most. It
427 suggests that the growth of phytoplankton community (predominantly coastal centric diatom
428 species) is primarily supported by intracellular Fe pools. Because such a low concentration of
429 [Fe(III)'] can not support the growth of coastal diatom species as stated earlier (Wells et al., 1994;
430 Soria-Dengg and Hortmann, 1995; Hutchins et al., 1999b; Wells, 1999; Maldonado and Price, 2001;
431 Wells and Trick, 2004). Under such conditions, a 20 μmol L^{-1} NO_3 drawdown primary using
432 intracellular Fe after the addition of DFB is a salient phenomenon observed in the present study (Fig.
433 7b-1). The increase in Chl *a* concentration in controls was greater than that in DFB treatment
434 probably due to the further Fe uptake from ambient seawater. Although the increase in diatom cell
435 density and species composition in both conditions were almost the same, the smaller increase in
436 Chl *a* concentration in DFB treatment than control would come from the reduced Chl *a* cell quota of
437 the diatoms under Fe-deficient condition. These *in situ* results are consistent with those in our
438 laboratory study with one order of magnitude higher Fe concentration. In addition, the decrease in
439 Chl *a* growth rate soon after the DFB addition may be due to the simultaneous degradation in
440 functional intracellular Fe pools and its distribution to daughter cells. The further increase in cell
441 density and Chl *a* concentration of the *in situ* phytoplankton community after the DFB addition was
442 probably due to NO_3+NO_2 and $Si(OH)_4$ depletions.

443 It is notable that, in comparison to the centric diatoms, pennate diatom species did not
444 undergo an increase in cell numbers to any prominent extent following the addition of DFB. This
445 suggests that the pennate diatoms, which could have the specific Fe-storage protein ferritin
446 (Marchetti et al., 2009), do not compete with centric diatoms in Fe-replete and hence
447 macronutrient-exhausted natural environments such as intensive spring phytoplankton bloom of the
448 Oyashio region (Sugie et al., 2010a). Species-specific difference in the strategy using intracellular
449 Fe may be one of the important factors controlling the diatom species composition after depletion of
450 extracellular bioavailable Fe in the spring bloom period. Our results suggest that the spring bloom

community of the Oyashio region dominated the centric diatoms could accumulate intracellular Fe relative to their critical threshold during winter to spring, when the high dissolved Fe concentration has been observed in the region (Nishioka et al., 2007; Nakayama et al., 2010). We also found that the intracellular Fe pools were used to increase cell numbers rather than Chl *a* production under Fe-depleted conditions of the Fe-starved diatom cells. A decrease in the concentration of intracellular Chl *a*, a main light-harvesting pigment could protect the Fe-starved cells from high irradiance which cause excess oxidative damages to the cells through photosynthesis (Ledford and Niyogi, 2005; Allen et al., 2008). The survival strategy may benefit to maximize the diatom dominance in the Oyashio region where Fe concentrations decrease with increasing irradiance toward summer (Nishioka et al., 2007).

Acknowledgements

We thank the captain, crews and colleagues aboard the R/V Hakuho-Maru KH07-01 cruise for their efforts and supports at sea. We also thank anonymous reviewers whose comments significantly improved this manuscript. This work was supported by grants for the Sasakawa Scientific Research Grant from the Japan Science Society to K. Sugie, for Scientific Research Project from the Research Institute for Humanity and Nature to K. Kuma, for Scientific Research (18201001) from the Ministry of Education, Culture, Sports, Science and Technology to K. Kuma, and from the Steel Industry Foundation for the Advancement of Environmental Protection Technology to K. Suzuki.

References

Allen AE, LaRoche J, Maheswari U, Lommer M, Schauer N, Lopez PJ, Finazzi G, Fernie AR, Bowler C (2008) Whole-cell response of the pennate diatom *Phaeodactylum tricornutum* to iron starvation. Proc Natl Acad Sci USA 105:10438–10443. doi:10.1073/pnas.0711370105

Anderson MA, Morel FMM (1982) The influence of aqueous iron chemistry on the uptake of iron by the coastal diatom *Thalassiosira weissflogii*. Limnol Oceanogr 27:789–813

Armbrust EV, Berges JA, Bowler C, Green BR, Martinez D, Putnam NH, Zhou S, Allen AE, Apt KE, Bechner M, Brzezinski MA, Chaal BK, Chiovitti A, Davis AK, Demarest MS, Detter JC, Glavina T, Goodstein D, Hadi MZ, Hellsten U, Hildebrand M, Jenkins BD, Jurka J, Kapitonov

481 VV, Kröger N, Lau WWY, Lane TW, Larimer FW, Lippmeier JC, Lucas S, Medina M,
482 Montsant A, Obornik M, Parker MS, Palenik B, Pazour GJ, Richardson PM, Rynearson TA,
483 Saito MA, Schwartz DC, Thamatrakoln K, Valentin K, Vardi A, Wilkerson FP, Rokhsar DS
484 (2004) The genome of the diatom *Thalassiosira pseudonana*: ecology, evolution, and
485 metabolism. Science 306:79–86
486 Brait JF, Curie C, Gaymard F (2007) Iron utilization and metabolism in plants. Curr Opin Plant Biol
487 10:276–282. doi:10.1016/j.pbi.2007.04.003
488 Busch A, Rimbauld B, Naumann B, RenschS, Hippler M (2008) Ferritin is required for rapid
489 remodeling of the photosynthetic apparatus and minimizes photo-oxidative stress in response
490 to iron availability in *Chlamydomonas reinhardtii*. Plant J 55:201–211.
491 doi:10.111/j.1365-313X.200803490.x
492 Chen M, Wang WX (2008) Accelerated uptake by phytoplankton of iron bound to humic acids.
493 Aquat Biol 3:155–166
494 Croot PL, Johansson M (2000) Determination of iron speciation by cathodic stripping voltammetry
495 in seawater using the competing ligand 2-(2-Thiazolylazo)-p-cresol (TAC). Electroanal
496 12:565–576
497 Davey M, Geider RJ (2001) Impact of iron limitation on the photosynthetic apparatus of the diatom
498 *Chaetoceros muelleri* (Bacillariophyceae). J Phycol 37:987–1000
499 Geider RJ, La Roche J (1994) The role of iron in phytoplankton photosynthesis, and the potential
500 for iron-limitation of primary productivity in the sea. Photosynth Res 39:275–301
501 Geider RJ, La Roche J, Greene RM, Olaizola M (1993) Response of the photosynthetic apparatus of
502 *Phaeodactylum tricornutum* (Bacillariophyceae) to nitrate, phosphate, or iron starvation. J
503 Phycol 29:755–766
504 Guillard RRL, Ryther JH (1962) Studies of marine planktonic diatoms. I. *Cyclotella nana* Hustedt
505 and *Detonula confervacea* (Gleve) Gran. Can J Microbiol 8:229–239
506 Hanawa K, Mitsudera H (1987) Variation of water system distribution in the Sanriku coastal area. J
507 Oceanogr Soc Jpn 42:435–446
508 Hasle GR (1978) Using the inverted microscope. In: Sournia A (ed) Phytoplankton manual,
509 UNESCO Monographs on Oceanographic Methodology 6. UNESCO, Paris, pp. 191–196
510 Hasle GR, Syvertsen EE (1997) Marine diatoms. In: Tomas CR (ed) Identifying Marine

511 Phytoplankton. Academic Press, London, pp. 5–385
512 Hassler CS, Schoemann V, Nichols CM, Butler ECV, Boyd PW (2011) Saccharides enhance iron
513 bioavailability to Southern Ocean phytoplankton. Proc Natl Acad Sci USA 108:1076–1081.
514 doi:10.1073/pnas.1010963108
515 Hattori-Saito A, Nishioka J, Ono T, McKay RML, Suzuki K (2010) Iron deficiency in micro-sized
516 diatoms in the Oyashio region of the western subarctic Pacific during spring. J Oceanogr
517 66:105–115
518 Hillebrand H, Durseien CD, Kirschtel D, Pollingher U, Zohary T (1999) Biovolume calculation for
519 pelagic and benthic microalgae. J Phycol 35:403–424
520 Hudson RJM, Morel FMM (1989) Distinguishing between extra- and intracellular iron in marine
521 phytoplankton. Limnol Oceanogr 34:1113–1120
522 Hudson RJM, Morel FMM (1990) Iron transport in marine phytoplankton: Kinetics of cellular and
523 medium coordination reactions. Limnol Oceanogr 35:1002–1020
524 Hudson RMJ, Covault DT, Morel FMM (1992) Investigations of iron coordination and redox
525 reactions in seawater using ^{59}Fe radiometry and ion-pair solvent extraction of amphiphilic iron
526 complexes. Mar Chem 38:209–235
527 Hutchins DA, Franck VM, Brzezinski MA (1999b) Inducing phytoplankton iron limitation in
528 iron-replete coastal waters with a strong chelating ligand. Limnol Oceanogr 44:1009–1018
529 Hutchins DA, Witter AE, Bulter A, Luther III GW (1999a) Competition among marine
530 phytoplankton for different cheleted iron species. Nature 400:858–861
531 Isada T, Hattori-Saito A, Saito H, Ikeda T, Suzuki K (2010) Primary productivity and its bio-optical
532 modeling in the Oyashio region, NW Pacific during the spring bloom 2007. Deep-Sea Res II
533 57:1653–1664. doi:10.1016/j.dsr2.2010.03.009
534 Iwade S, Kuma K, Isoda Y, Yoshida M, Kudo I, Nishioka J, Suzuki K (2006) Effect of high iron
535 concentrations on iron uptake and growth of a coastal diatom *Chaetoceros sociale*. Aquat
536 Microb Ecol 43:177–191
537 Ledford HK, Niyogi KK (2005) Singlet oxygen and photo-oxidative stress management in plants
538 and algae. Plant Cell Env 28:1037–1045
539 Kono T, Sato M (2010) A mixing analysis of surface water in the Oyashio region: Its implications
540 and application to variations of the spring bloom. Deep-Sea Res II 57:1595–1607.

541 doi:10.1016/j.dsr2.2010.03.004
542 Kuma K, Matsunaga K (1995) Availability of colloidal ferric oxides to coastal marine
543 phytoplankton. Mar Biol 122:1–11
544 Kuma K, Nishioka J, Matsunaga K (1996) Controls on iron(III) hydroxide solubility in seawater:
545 The influence of pH and natural organic chelators. Limnol Oceanogr 41:396–407
546 Kuma K, Tanaka J, Matsunaga K (1999) Effect of natural and synthetic organic-Fe(III) complexes
547 in an estuarine mixing model on iron uptake and growth of a coastal marine diatom,
548 *Chaetoceros sociale*. Mar Biol 134:761–769
549 Kuma K, Tanaka J, Matsunaga K, Matsunaga K (2000) Effect of hydroxamate ferrisiderophore
550 complex (ferrichrome) on iron uptake and growth of a coastal marine diatom, *Chaetoceros*
551 *sociale*. Limnol Oceanogr 45:1235–1244
552 Kustka AB, Allen AE, Morel FMM (2007) Sequence analysis and transcriptional regulation of iron
553 acquisition genes in two marine diatoms. J Phycol 43:715–729.
554 doi:10.1111/j.1529-8817.2007.00359.x
555 Maldonado MT, Price NM (2001) Reduction and transport of organically bound iron by
556 *Thalassiosira oceanica* (Bacillariophyceae). J Phycol 37:298–309
557 Marchetti A, Harrison PJ (2007) Coupled changes in the cell morphology and the elemental (C, N,
558 and Si) composition of the pennate diatom *Pseudo-nitzschia* due to iron deficiency. Limnol
559 Oceanogr 52:2270–2284
560 Marchetti A, Parker MS, Moccia LP, Lin EO, Arrieta AL, Ribalet F, Murphy MEP, Maldonado MT,
561 Armbrust EV (2009) Ferritin is used for iron storage in bloom-forming marine pennate
562 diatoms. Nature 457:467–470. doi:10.1038/nature07539
563 Morel FMM, Rueter JG, Anderson DM, Guillard RRL (1979) AQUIL: A chemically defined
564 phytoplankton culture medium for trace metal studies. J Phycol 15:135–141
565 Morel FMM, Kustka AB, Shaked Y (2008) The role of unchelated Fe in the iron nutrition of
566 phytoplankton. Limnol Oceanogr 53:400–404
567 Moseley JL, Allinger T, Herzog S, Hoerth P, Wehinger E, Merchant S, Hippler M (2002) Adaptation
568 to Fe-deficiency requires remodeling of the photosynthetic apparatus. EMBO J 21:6709–6720
569 Nakayama Y, Kuma K, Fujita S, Sugie K, Ikeda T (2010) Temporal variability and bioavailability of
570 iron and nutrient during spring phytoplankton bloom in the Oyashio region. Deep-Sea Res II

571 57:1618–1642. doi:10.1016/j.dsr2.2010.03.006
572 Nishioka J, Ono T, Saito H, Nakatsuka T, Takeda S, Yoshimura T, Suzuki K, Kuma K, Nakabayashi
573 S, Tsumune D, Mitsudera H, Johnson WK, Tsuda A (2007) Iron supply to the western subarctic
574 Pacific: Importance of iron export from the Sea of Okhotsk. J Geophys Res 112 C10012.
575 doi:10.1029/2006JC004055
576 Obata H, Karatani H, Nakayama E (1993) Automated determination of iron in seawater by chelating
577 resin concentration and chemiluminescence detection. Anal Chem 65:1524–1528
578 Peers G, Price NM (2004) A role for manganese in superoxide dismutases and growth of
579 iron-deficient diatoms. Limnol Oceanogr 49:1774–1783
580 Raven JA (1988) The iron and molybdenum use efficiencies of plant growth with different energy,
581 carbon and nitrogen sources. New Phytol 109:279–287
582 Raven JA (1997) The vacuole: a cost-benefit analysis. Adv Bot Res 25:59–86
583 Raven JA, Evans MCW, Korb RE (1999) The role of trace metals in photosynthetic electron
584 transport in O_2-evolving organisms. Photosynth Res 60:111–149
585 Rue EL, Bruland KW (1995) Complexation of iron(III) by natural organic ligands in the Central
586 North Pacific as determined by a new competitive ligand equilibration / adsorptive cathodic
587 stripping voltammetric method. Mar Chem 50:117–138
588 Shaked Y, Kustka AB, Morel FMM (2005) A general kinetic model for iron acquisition by
589 eukaryotic phytoplankton. Limnol Oceanogr 50:872–882
590 Soria-Dengg S, Horstmann U (1995) Ferrioxamines B and E as iron sources for the marine diatom
591 *Phaeodactylum tricornutum*. Mar Ecol Prog Ser 127:269–277
592 Stumm W, Morgan JJ (1996) Aquatic Chemistry, 3rd ed. Wiley InterScience, New York, pp.1022
593 Sugie K, Kuma K (2008) Resting spore formation in the marine diatom *Thalassiosira*
594 *nordenskioeldii* under iron- and nitrogen-limited conditions. J Plankton Res 30:1245–1255.
595 doi:10.1093/plankt/fbn080
596 Sugie K, Kuma K, Fujita S, Ikeda T (2010b) Increase in Si:N drawdown ratio due to resting spore
597 formation by spring bloom-forming diatoms under Fe- and N-limited conditions in the Oyashio
598 region. J Exp Mar Biol Ecol 382:108–116. doi:10.1016/j.jembe.2009.11.001
599 Sugie K, Kuma K, Fujita S, Nakayama Y, Ikeda T (2010a) Nutrient and diatom dynamics during
600 late winter and spring in the Oyashio region of the western subarctic Pacific Ocean. Deep-Sea

601 Res II 57:1630–1642. doi:10.1016/j.dsr2.2010.03.007
602 Sun J, Liu D (2003) Geometric models for calculating cell biovolume and surface area for
603 phytoplankton. J Plankton Res 25:1331–1346
604 Sunda WG (2001) Bioavailability and bioaccumulation of iron in the sea. In: Turner DR, Hunter
605 KA (eds) The biogeochemistry of iron in seawater. Wiley, New York, pp. 41–84
606 Sunda WG, Huntsman SA (1995) Iron uptake and growth limitation in oceanic and coastal
607 phytoplankton. Mar Chem 50:189–206
608 Sunda WG, Huntsman SA (1997) Interrelated influence of iron, light and cell size on marine
609 phytoplankton growth. Nature 390:389–392
610 Suzuki R, Ishimaru T (1990) An improved method for the determination of phytoplankton
611 chlorophyll using N, N-dimethylformamide. J Oceanogr Soc Jpn 46:190–194
612 Takeda S, Obata H (1995) Response of equatorial Pacific phytoplankton to subnanomolar Fe
613 enrichment. Mar Chem 50:219-227
614 Terzulli A, Kosman DJ (2010) Analysis of the high-affinity iron uptake system at the
615 *Chlamydomonas reinhardtii* plasma membrane. Eukaryot Cell 9:815–826.
616 doi:10.1128/EC.00310-09
617 Tsuda A, Kiyosawa H, Kuwata A, Mochizuki M, Shiga N, Saito H, Chiba S, Imai K, Nishioka J,
618 Ono T (2005) Responses of diatoms to iron-enrichment (SEEDS) in the western subarctic
619 Pacific, temporal and spatial comparisons. Prog Oceanogr 64:189–205.
620 doi:10.1016/j.pocean.2005.02.008
621 Ushizaka S, Sugie K, Yamada M, Kasahara M, Kuma K (2008) Significance of Mn and Fe for the
622 growth of a coastal marine diatom, *Thalassiosira weissflogii*. Fisheries Sci 74:1137–1145.
623 doi:10.111/j.1444-2906.2008.01633.x
624 Wells ML (1999) Manipulating iron availability in nearshore waters. Limnol Oceanogr
625 44:1002–1008
626 Wells ML, Price NM, Bruland KW (1994) Iron limitation and the cyanobacterium *Synechococcus* in
627 equatorial Pacific waters. Limnol Oceanogr 39:1481–1486
628 Wells ML, Trick CG (2004) Controlling iron availability to phytoplankton in iron-replete coastal
629 waters. Mar Chem 86:1–13. doi:10.1016/j.marchem.2003.10.003
630 Welschmeyer NA (1994) Fluorometric analysis of chlorophyll *a* in the present of chlorophyll *b* and

pheopigments. Limnol Oceanogr 39:1985–1992

Witter AE, Hutchins DA, Butler A, Luther III GW (2000) Determination of conditional stability constants and kinetic constants for strong model Fe-binding ligands in seawater. Mar Chem 69:1–17

Yoshida M, Kuma K, Iwade S, Isoda Y, Takata H, Yamada M (2006) Effect of aging time on the availability of freshly precipitated ferric hydroxide to coastal marine diatoms. Mar Biol 149:379–392. doi:10.1007/s00227-005-0187-y

Yun CW, Ferea T, Rashford J, Ardon O, Brown PO, Botstein D, Kaplan J, Philpott CC (2000) Desferrioxamine-mediated iron uptake in *Saccharomyces cerevisiae*. Evidence for two pathways of iron uptake. J Biol Chem 275:10709–10715

Table and Figure legends

Table 1. Experimental condition of seven treatments to examine the ability for luxury Fe uptake and the potential for growth utilizing intracellular Fe pools for *Skeletonema costatum* s.l., *Thalassiosira anguste-lineata*, *Thalassiosira nordenskioeldii* and *Thalassiosira weissflogii*. Note that the direct Fe(III)-10 and direct Fe(III)-10-DFB-1d treatments were not conducted using *T. anguste-lineata*.

Table 2. Cell size of coastal diatom species at the start (S) and end (E) of Fe-limited culture experiment in direct Fe-100-DFB-1d medium with 100-nmol L^{-1} Fe(III) to which DFB (desferrioxamine B) was added after incubation for 1 day [DFB:Fe(III) = 10:1]. Data represent the mean ± 1 SD ($n \geq 20$). *: Significant difference of $p < 0.01$ in ANOVA between the value of the start and the end.

Fig. 1. *Thalassiosira nordenskioeldii* (10°C). Changes in cell density (a) and Chl *a* concentration (b) of cultures in direct Fe(III) input media with 10 and 100-nmol L^{-1} Fe(III) [direct Fe(III)-10 and direct Fe(III)-100 media, respectively], direct Fe(III) input media with addition of DFB [DFB:Fe(III) = 10:1] after 1 day cultivation (direct Fe-10-DFB-1d and direct Fe-100-DFB-1d media, respectively), premixed DFB-Fe(III) complex [DFB:Fe(III) = 1-μmol L^{-1}:100-nmol L^{-1}] and control (only DFB addition with a final concentration of 1-μmol L^{-1}) media. Data on cell and Chl *a* concentrations represent mean ± 1 SD for triplicate cultivations other than duplicate ± range of control and premix DFB-Fe(III) treatments. Dashed lines in (a-1) and (b-1) represent maximum values of vertical axes in (a-2) and (b-2), respectively.

Fig. 2. *Thalassiosira anguste-linieata* (10°C). Changes in cell density (a) and Chl *a* concentration (b). Experimental treatments and figure captions were the same as those in Fig. 1.

Fig. 3. *Skeletonema costatum* s.l. (20°C). Changes in cell density (a) and Chl *a* concentration (b). Experimental treatments and figure captions were the same as those in Fig. 1.

Fig. 4. *Thalassiosira weissflogii* (20°C). Changes in cell density (a) and Chl *a* concentration (b). Experimental treatments and figure captions were the same as those in Fig. 1.

691

692 **Fig. 5**. Change in cell densities of *T. nordenskioeldii* at 10°C (a), *T. anguste-lineata* at 10°C (b), *S.*
693 *costatum* s.l. at 20°C (c) and *T. weissflogii* at 20°C (d) in direct Fe(III)-100 media without and with
694 addition of DFB after 1 and 3 day of cultivations [direct Fe(III)-100, direct Fe-100-DFB-1d and
695 direct Fe-100-DFB-3d treatment]. Data on cell concentration represent mean ± 1 SD for triplicate
696 cultivations.

697

698 **Fig. 6**. Maximum cell divisions [$\log_2$ (maximal cell density after DFB addition/cell density at DFB
699 addition)] and Chl *a* doublings [$\log_2$ (maximal Chl *a* concentration after DFB addition/Chl *a*
700 concentration at DFB addition)] of *T. nordenskioeldii* (10°C), *T. anguste-lineata* (10°C), *S. costatum*
701 s.l. (20°C) and *T. weissflogii* (20°C) in direct Fe(III)-100 input with addition of DFB [DFB:Fe(III) =
702 10:1] after 1 day of cultivation (direct Fe-100-DFB-1d medium, Fig. 1a-2, 1b-2, 2a-2, 2b-2, 3-a2,
703 3b-2, 4a-2 and 4b-2) in laboratory culture experiments. Error bars on cell divisions and Chl *a*
704 doublings represent mean ± 1 SD for triplicate cultivations.

705

706 **Fig. 7**. Changes in Chl *a* concentration (a-1), diatom density (a-2) and nutrient concentrations
707 [NO_3+NO_2 (b-1), PO_4 (b-2), $Si(OH)_4$ (b-3)] at 0, 1, 3 and/or 5 day cultivations in the shipboard
708 incubation experiments. Data on Chl *a* and nutrient concentrations represent mean ± 1 SD for
709 triplicate cultivations.

710

711 **Fig. 8**. Changes in Chl *a* cell quota (Chl *a* concentration/cell density at each point) of *T.*
712 *nordenskioeldii* (a), *T. anguste-lineata* (b), *S. costatum* s.l. (c) and *T. weissflogii* (d) with incubation
713 time in direct Fe(III) input media with 10 and/or 100-nmol L^{-1} Fe(III) [direct Fe(III)-10 and/or
714 direct Fe(III)-100 media, respectively] and direct Fe(III) input media with addition of DFB
715 [DFB:Fe(III) = 10:1] after 1 day cultivation (direct Fe-10-DFB-1d and/or direct Fe-100-DFB-1d
716 media, respectively). Data represent mean ± 1 SD for triplicate cultivations.

717

718

719

720

721 和文要旨

722 Importance of Intracellular Fe Pools on Growth of Marine Diatoms by Using Unialgal Cultures and
723 the Oyashio Region Phytoplankton Community during Spring

724 Koji Sugie, Kenshi Kuma, Satoshi Fujita, Satomi Ushizaka, Koji Suzuki and Tsutomu Ikeda

725 邦題：珪藻の単離培養株および春季親潮域の植物プランクトン群集の増殖における細胞内
726 鉄プール利用の重要性

727 杉江　恒二, 久万　健志, 藤田　聡, 牛坂　理美, 鈴木　光次, 池田　勉

728 　沿岸性中心目珪藻 4 種の単離培養株および親潮域の天然植物プランクトン群集を用いて,
729 高鉄濃度環境下における過剰量の鉄摂取能および細胞内の鉄を利用した増殖能に関して調
730 査した。全ての単離株は細胞内の鉄のみを利用することにより 2.4–4.2 回の細胞分裂を行っ
731 ていた。一方，クロロフィル *a*（Chl *a*）の増加は 1.2–2.6 回分裂相当であり細胞の増分と比
732 較して少なかった。すなわち，鉄欠乏環境にある珪藻は細胞内の鉄を Chl *a* の生産ではな
733 く細胞数の増大のために利用していた。天然群集を用いた船上試験においても単離株の結
734 果と同様の傾向を示し，細胞数の増分が Chl *a* の増分を上回った。鉄が枯渇した環境にお
735 いて，珪藻細胞内の Chl *a* 量を優先的に減少させることは光酸化損傷を引き起こす高照度
736 環境下から細胞を守るための良い生存戦略となるかもしれない。そのような海水中の低鉄
737 濃度，高照度環境は春季から夏季の親潮域において頻繁に発生すると考えられる。

Table 1. Experimental condition of seven treatments to examine the ability for luxury Fe uptake and the potential for growth utilizing intracellular Fe pools for *Skeletonema costatum* s.l., *Thalassiosira anguste-lineata*, *Thalassiosira nordenskioeldii* and *Thalassiosira weissflogii*. Note that the direct Fe(III)-10 and direct Fe(III)-10-DFB-1d treatments were not conducted using *T. anguste-lineata*.

Treatment	Added Fe(III) (nmol L^{-1})	Added DFB (nmol L^{-1})	Time of DFB addition (day)
Control (DFB)	0	1000	0
Premixed DFB-Fe(III)	100	1000	0
Direct Fe(III)-10	10	0	No add.
Direct Fe(III)-100	100	0	No add.
Direct Fe(III)-10-DFB-1d	10	100	1
Direct Fe(III)-100-DFB-1d	100	1000	1
Direct Fe(III)-100-DFB-3d	100	1000	3

Table 2. Cell size of coastal diatom species at the start (S) and end (E) of Fe-limited culture experiment in direct Fe-100-DFB-1d medium with 100-nmol L^{-1} Fe(III) to which DFB (desferrioxamine B) was added after incubation for 1 day [DFB:Fe(III) = 10:1]. Data represent the mean ± 1 SD (n≥20). *: significant difference of $p < 0.01$ in ANOVA between the value of the start and the end.

Species	Start (S) or end (E) of culture	Cell volume (CV: μm^3)	Cell surface area (SA: μm^2)	SA/CV (μm^{-1})
T. nordenskioeldii	(S)	4,400 ± 49	1,520 ± 110	0.35 ± 0.01
	(E)	3,730 ± 620*	1,390 ± 160*	0.38 ± 0.02*
T. anguste-lineata	(S)	10,570 ± 1,740	2,800 ± 260	0.27 ± 0.02
	(E)	8,620 ± 1,600*	2,470 ± 310*	0.29 ± 0.02*
S. costatum s.l.	(S)	117 ± 33	81 ± 15	0.71 ± 0.07
	(E)	194 ± 101*	136 ± 57*	0.73 ± 0.09
T. weissflogii	(S)	518 ± 98	358 ± 45	0.70 ± 0.05
	(E)	415 ± 124*	308 ± 60*	0.76 ± 0.07*

Fig. 1

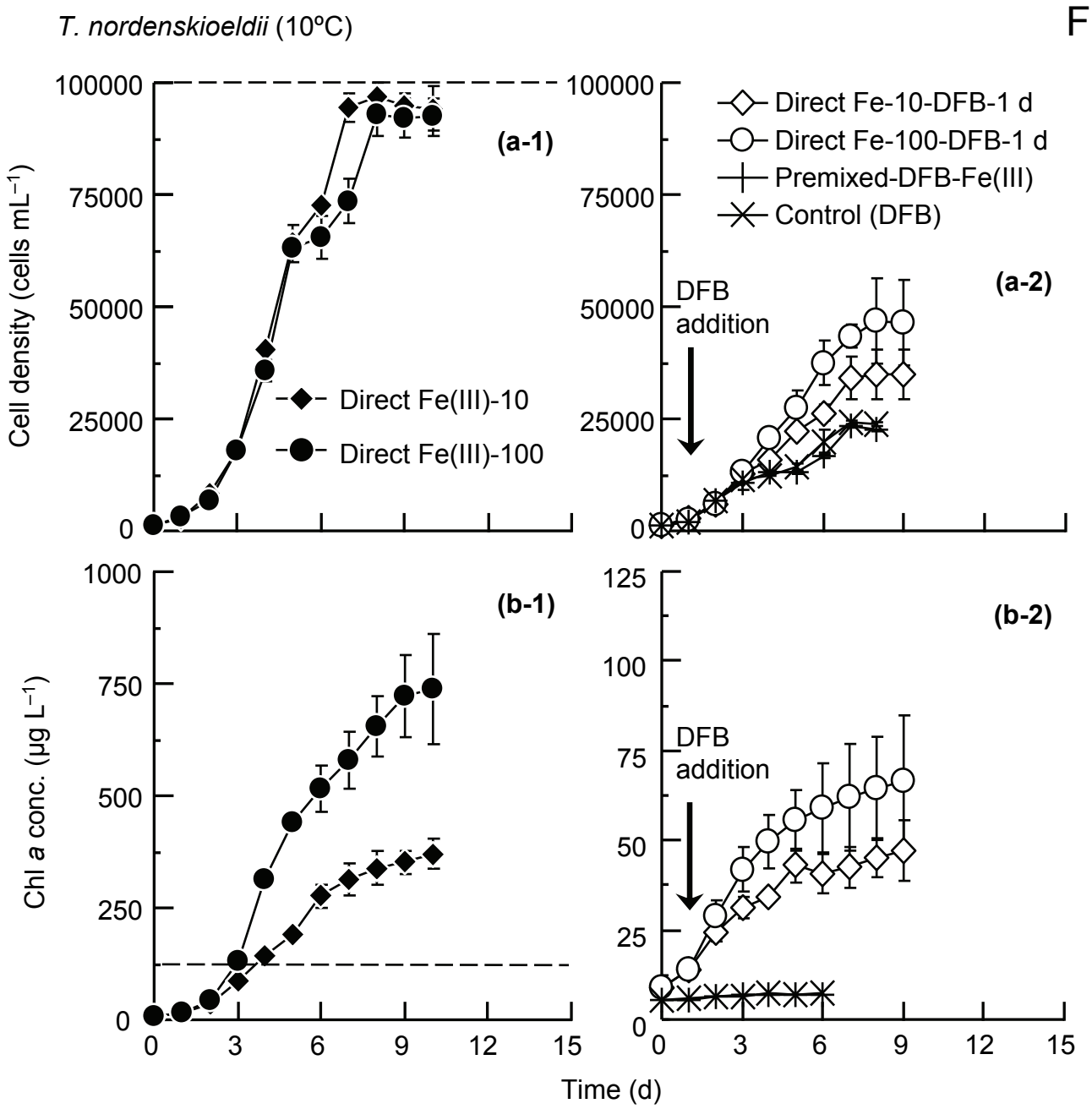
T. nordenskioeldii (10ºC)
(a-1)
(a-2)
(b-1)
(b-2)
Cell density (cells mL^{-1})
Chl *a* conc. (µg L^{-1})
Time (d)
Direct Fe(III)-10
Direct Fe(III)-100
Direct Fe-10-DFB-1 d
Direct Fe-100-DFB-1 d
Premixed-DFB-Fe(III)
Control (DFB)
DFB addition
DFB addition
0
25000
50000
75000
100000
250
500
750
1000
25
50
75
100
125
0
3
6
9
12
15

Fig. 2

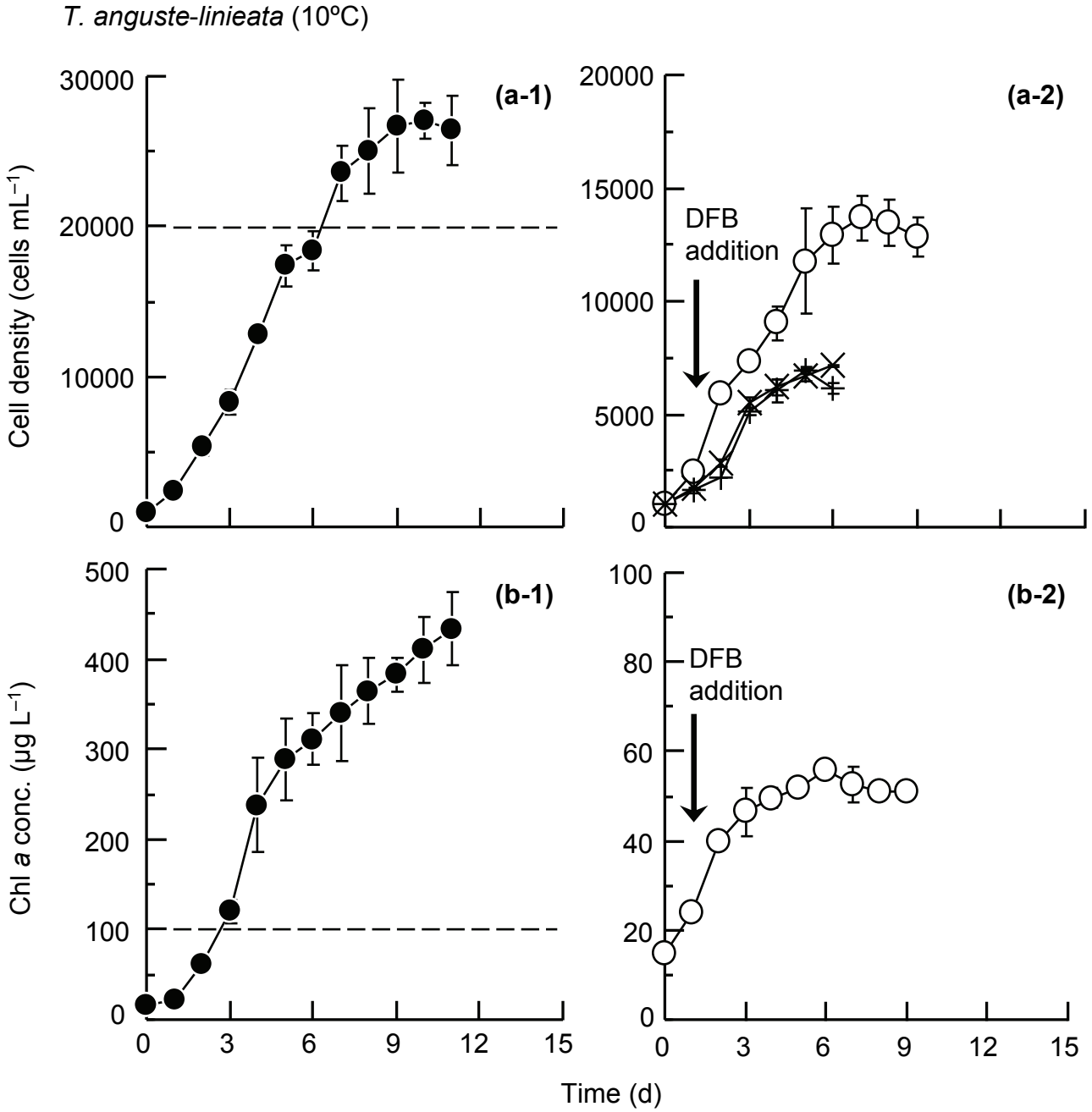
T. anguste-linieata (10ºC)
(a-1)
(a-2)
(b-1)
(b-2)
DFB addition
DFB addition
Cell density (cells mL−1)
Chl a conc. (µg L−1)
Time (d)
30000
20000
10000
0
20000
15000
10000
5000
0
500
400
300
200
100
0
100
80
60
40
20
0
0
3
6
9
12
15

Fig. 3

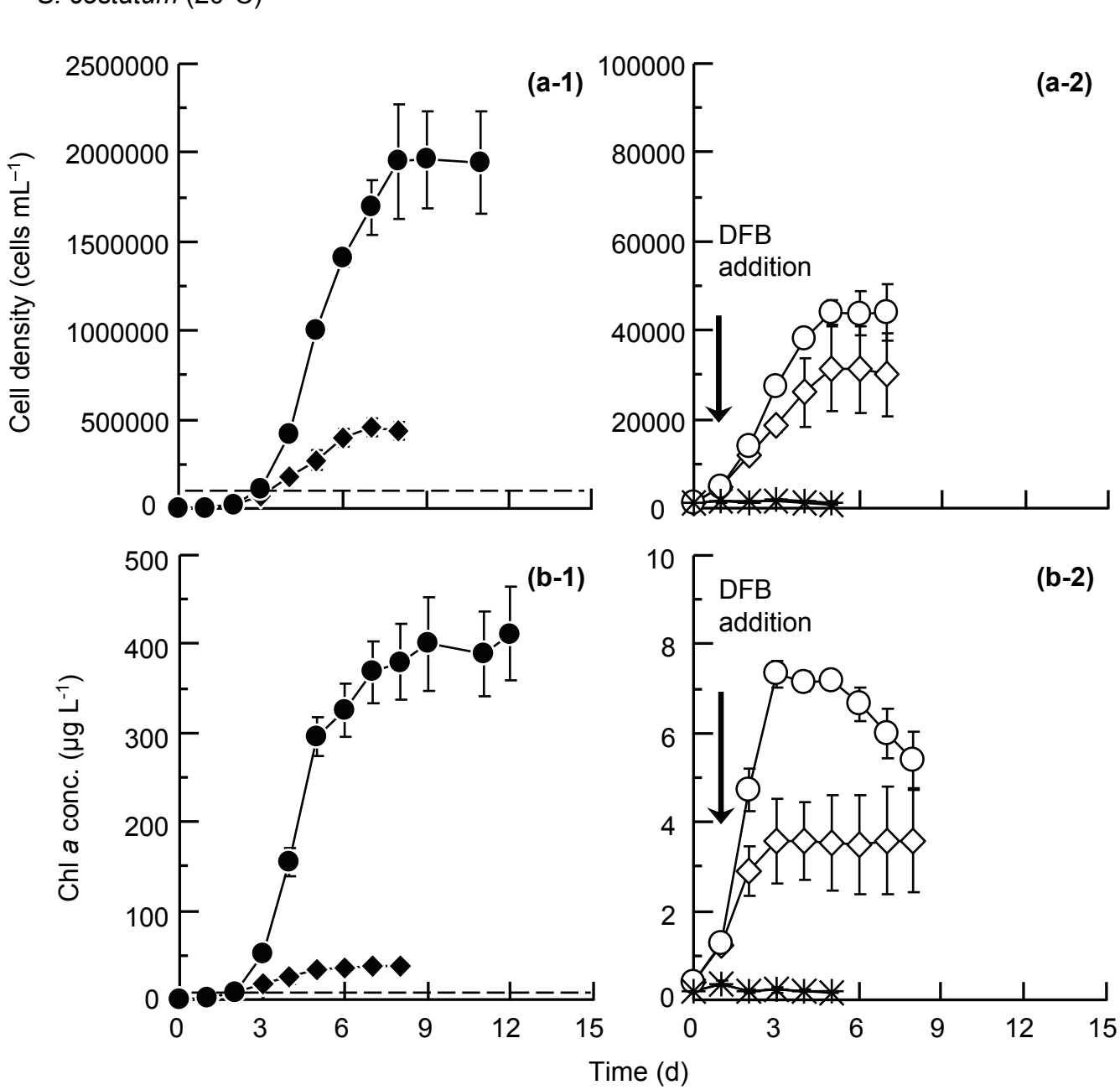
S. costatum (20ºC)
(a-1)
(a-2)
(b-1)
(b-2)
DFB addition
DFB addition
Cell density (cells mL−1)
Chl a conc. (µg L-1)
Time (d)
2500000
2000000
1500000
1000000
500000
0
100000
80000
60000
40000
20000
500
400
300
200
100
10
8
6
4
2
0 3 6 9 12 15

T. weissflogii (20ºC)

Fig. 4

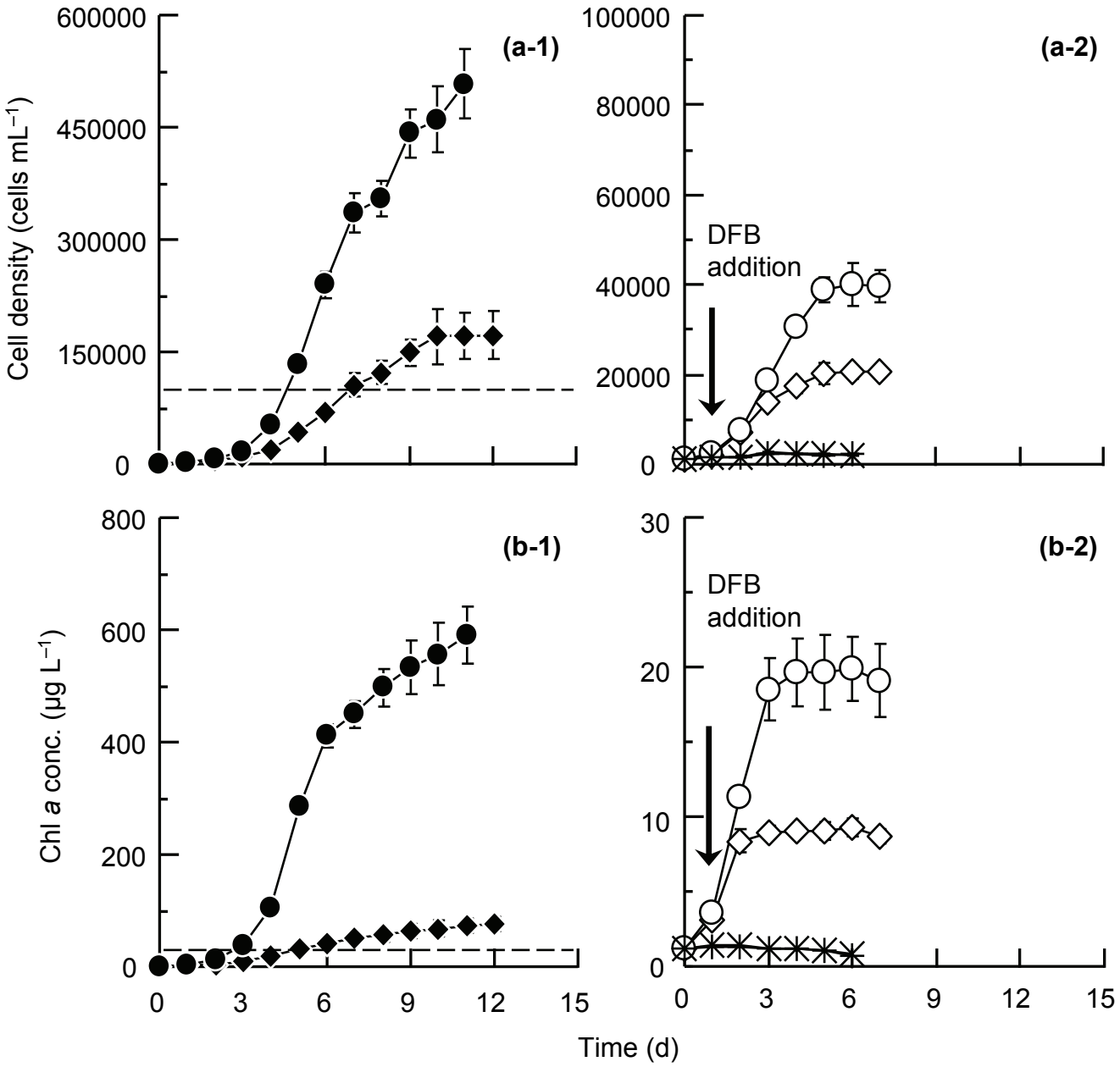

Fig. 5

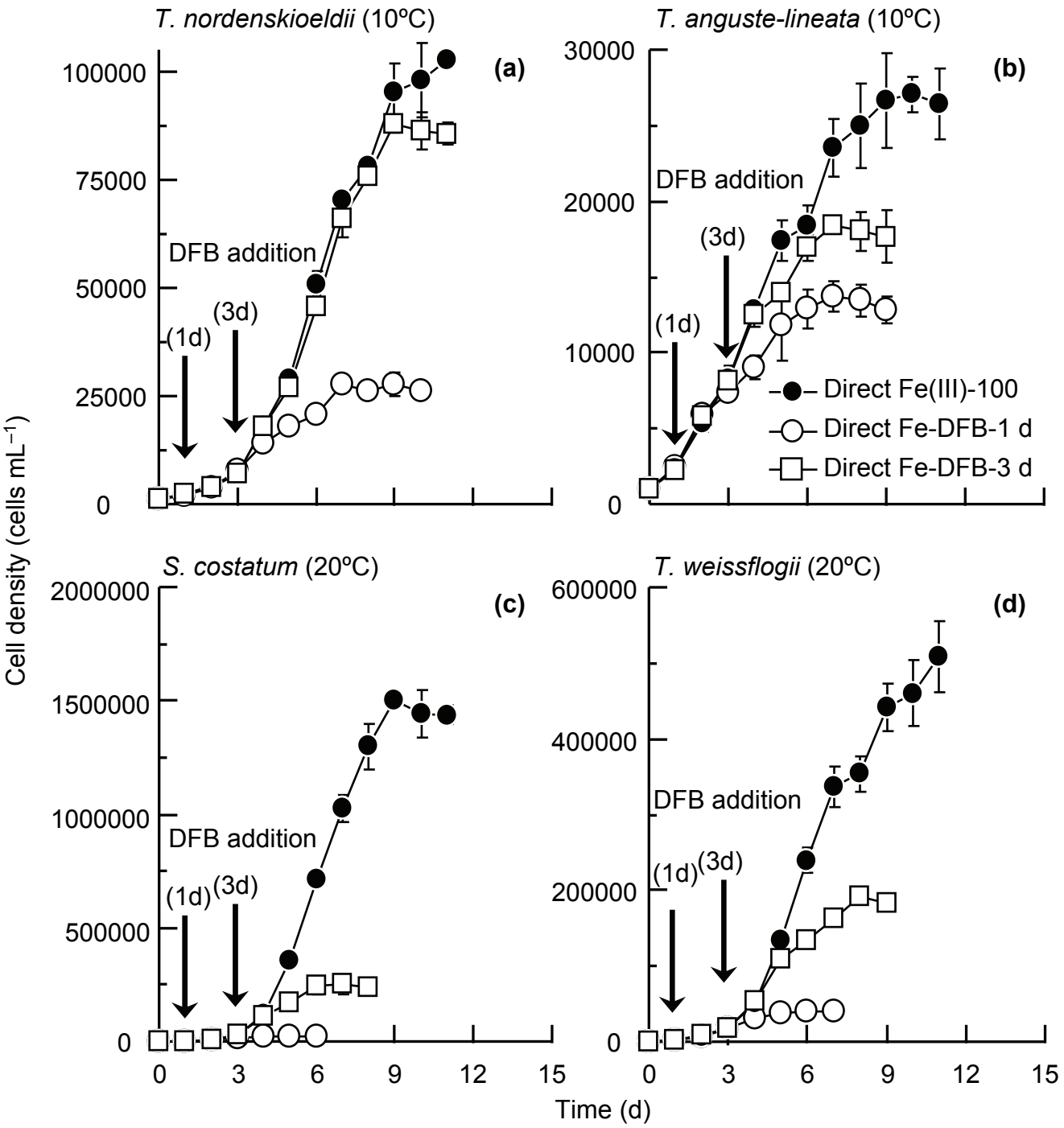
T. nordenskioeldii (10ºC)
(a)
100000
75000
50000
25000
0
DFB addition
(1d)
(3d)
T. anguste-lineata (10ºC)
(b)
30000
20000
10000
0
DFB addition
(1d)
(3d)
Direct Fe(III)-100
Direct Fe-DFB-1 d
Direct Fe-DFB-3 d
S. costatum (20ºC)
(c)
2000000
1500000
1000000
500000
0
DFB addition
(1d)
(3d)
T. weissflogii (20ºC)
(d)
600000
400000
200000
0
DFB addition
(1d)
(3d)
0
3
6
9
12
15
Time (d)
Cell density (cells mL−1)

Fig. 6

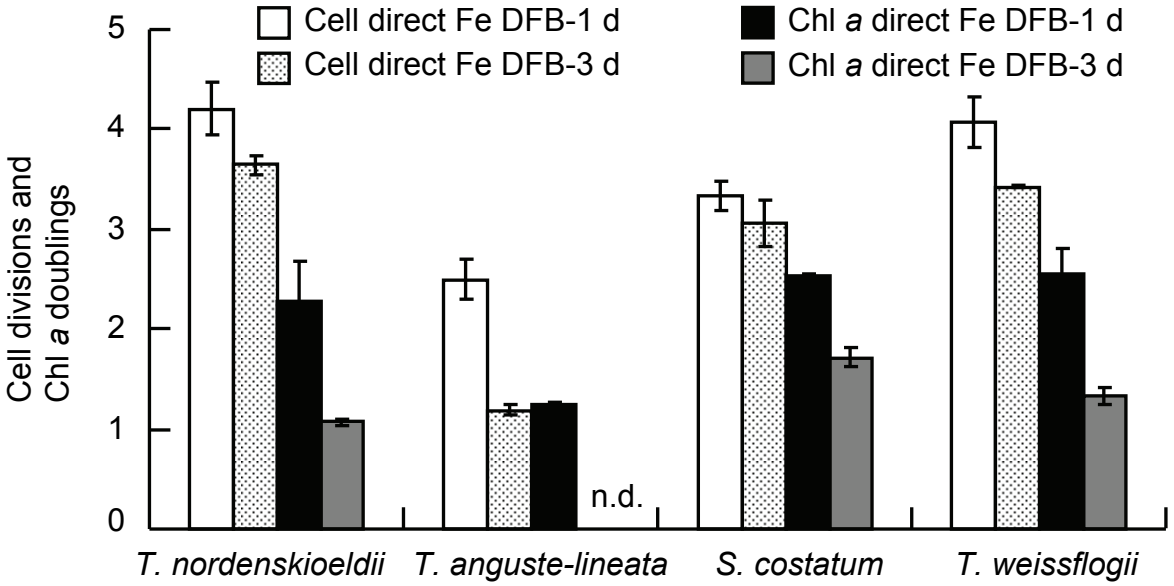
Cell direct Fe DFB-1 d
Cell direct Fe DFB-3 d
Chl *a* direct Fe DFB-1 d
Chl *a* direct Fe DFB-3 d
Cell divisions and Chl *a* doublings
0
1
2
3
4
5
n.d.
T. nordenskioeldii
T. anguste-lineata
S. costatum
T. weissflogii

Fig. 7

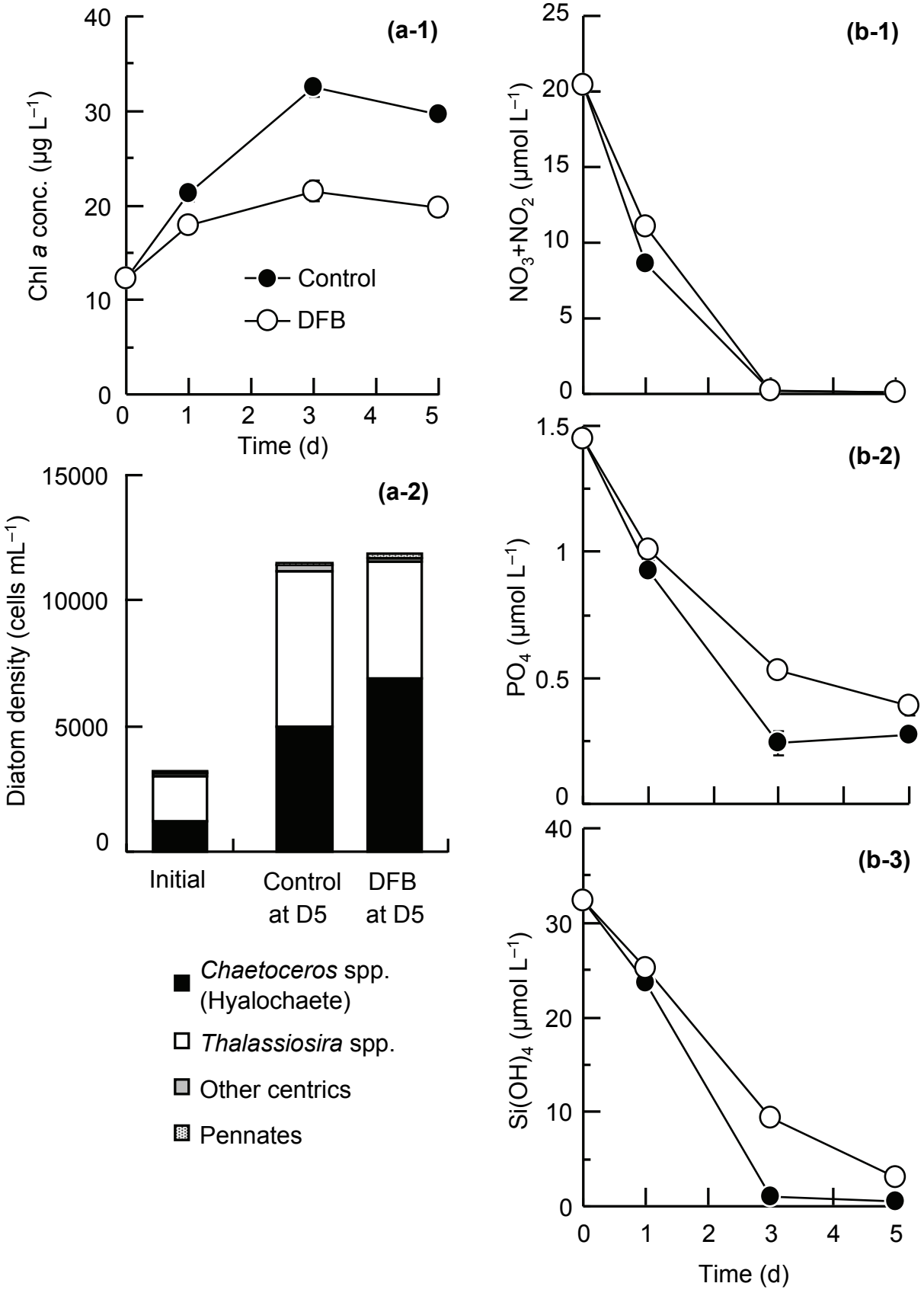
(a-1)
Chl a conc. (μg L−1)
Time (d)
Control
DFB
(a-2)
Diatom density (cells mL−1)
Initial
Control at D5
DFB at D5
Chaetoceros spp. (Hyalochaete)
Thalassiosira spp.
Other centrics
Pennates
(b-1)
NO3+NO2 (μmol L−1)
(b-2)
PO4 (μmol L−1)
(b-3)
Si(OH)4 (μmol L−1)
Time (d)

Fig. 8

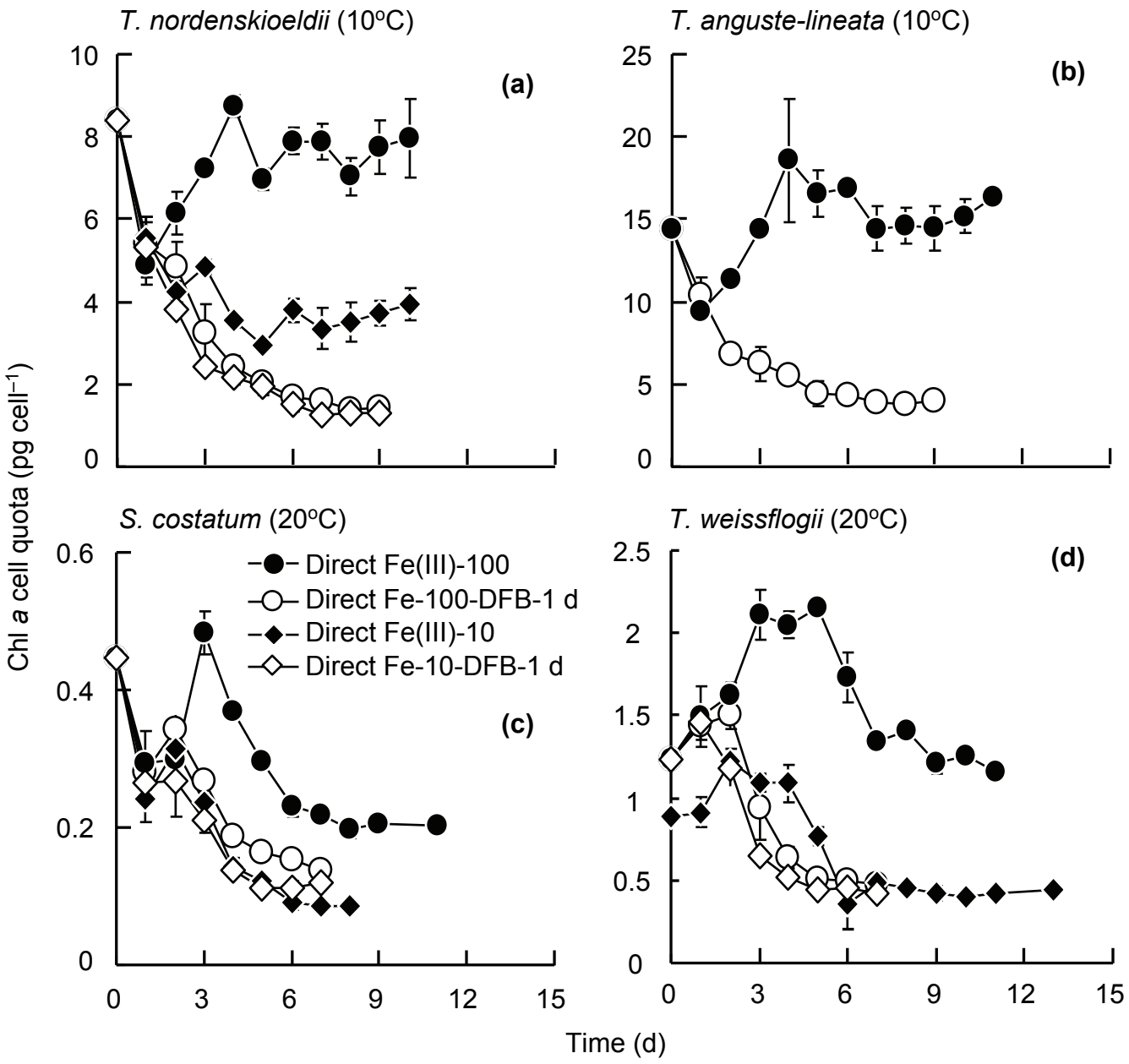
T. nordenskioeldii (10°C)
(a)
T. anguste-lineata (10°C)
(b)
S. costatum (20°C)
(c)
T. weissflogii (20°C)
(d)
Direct Fe(III)-100
Direct Fe-100-DFB-1 d
Direct Fe(III)-10
Direct Fe-10-DFB-1 d
Chl a cell quota (pg cell⁻¹)
Time (d)